Metallomics

RSC Publishing

PAPER

View Article Online
View Journal | View Issue

Cite this: *Metallomics*, 2013, **5**, 913

Cellular response of *E. coli* upon Hg^{2+} exposure – a case study of advanced nuclear analytical approach to metalloproteomics

Yuxi Gao,[a] Xiaomin Peng,[ab] Jinchao Zhang,*[b] Jiating Zhao,[a] Yunyun Li,[a] Yufeng Li,[a] Bai Li,[a] Yi Hu*[a] and Zhifang Chai[a]

The response of *E. coli* to Hg^{2+} exposure was investigated using proteomic and metalloproteomic approaches. *E. coli* was cultured in the LB medium containing $HgCl_2$ and/or selenomethionine. The growth curve of *E. coli* was measured to estimate the toxicity of Hg^{2+} or selenomethionine. After two-dimensional gel electrophoresis (2-DE), distribution of Hg in 2-DE gel was detected with synchrotron radiation X-ray fluorescence (SRXRF) at 4W1B, Beijing Synchrotron Radiation Facility. The proteins with differential expression and those containing Hg were identified with electrospray ionization tandem mass spectrometry (ESI-MS/MS) and peptide mass fingerprinting analysis. The results showed that Hg^{2+} can inhibit the growth of *E. coli*, while supplement of selenomethionine can shorten the lag period induced by Hg^{2+}, indicating an antagonistic effect of selenomethionine against Hg^{2+} toxicity. Mechanistically, Hg was observed to be able to bind pyruvate kinase, a glycolytic enzyme, and modulate the expression of five other proteins, including down-regulation of outer membrane protein W and up-regulation of transcription termination factor rho, cysteine synthase, transaldolase A and alkyl hydroperoxide reductase subunit C. Therefore, our results indicated that mercury may influence osmosis of plasma membrane, antioxidant defense, and glycometabolism of the microorganism. This study demonstrates the high sensitivity of SRXRF in identifying metal-associated proteins compared to conventional proteomic approaches.

Received 31st December 2012,
Accepted 23rd May 2013

DOI: 10.1039/c3mt20279h

www.rsc.org/metallomics

Introduction

Mercury (Hg) is listed as one of the most dangerous chemicals by the International Program of Chemical Safety. Due to its ability to undergo methylation, accumulation, and biomagnification in food chains, the threat of Hg to human health has received considerable attention.[1,2] Hg can accumulate in the human body and is toxic to the kidneys, central nervous system, cardiovascular, gastrointestinal, and immune systems.[3–5] Tissue toxicity of Hg largely depends on the chemical forms of Hg. For instance, prenatal exposure to organic Hg, which can penetrate the blood–brain barrier, severely affects the neurobehavioral functioning of offspring.[3] The cellular toxicity of Hg is believed to be due to its high affinity for thiols in proteins.[6] Both Hg^{2+} and methylmercury (MeHg) can form covalent bonds with glutathione (GSH) or the cysteine, cystine, methionine and taurine residues of proteins, which results in disturbed GSH metabolism, protein inactivation and cell damage.[7] Hg can also produce free radicals in cells and induce lipid, protein, or DNA oxidation.[8–13] Despite extensive research of Hg over the past several decades, detailed mechanisms accounting for cellular toxicity of Hg remain poorly understood and further research in this area is highly desirable.[14]

As metals can generally modulate a complex array of proteins, a proteomic approach that is capable of identifying Hg-related proteins in cells would be useful for dissecting Hg toxicity.[15–17] In the past decade, conventional proteomic studies of protein expression levels have been conducted to examine how Hg exerts its toxic effects in biological systems and how organisms are acclimatized to Hg stress. For instance, Chen and colleagues[18] had employed two-dimensional gel electrophoresis (2-DE), coupled with electrospray ionization

[a] *CAS Key Laboratory of Nuclear Analytical Techniques, Key Laboratory for Biomedical Effects of Nanomaterials and Nanosafety, Institute of High Energy Physics, Chinese Academy of Sciences (CAS), Beijing 100049, China. E-mail: huyi@ihep.ac.cn; Fax: +86 010 88233212; Tel: +86 010 88233212*

[b] *Key Laboratory of Chemical Biology of Hebei Province, College of Chemistry and Environmental Science, Hebei University, Baoding, Hebei 071002, China. E-mail: jczhang6970@yahoo.com.cn; Fax: +86 0312 5079005; Tel: +86 0312 5079005*

tandem mass spectrometry (ESI-MS/MS), to investigate proteomic changes in rice roots under Hg stress. They found 25 proteins spots differentially expressed in rice roots and altered activity of redox enzymes, including superoxide dismutase (SOD), catalase (CAT) and peroxidase (POD), arising from Hg exposure.[18] Similar methodologies have also been applied to microorganisms to identify the proteins differentially expressed upon exposure to Hg or other heavy metals.[14,19,20] In humans, blood plasma and serum samples from 34 children were collected to analyze the effects of Hg and Pb exposure at concentrations well below Centers for Disease Control and Prevention (CDC) guidelines.[21] After depleting the most abundant proteins using antibody-based affinity columns, 16 proteins in children's blood have been identified to be potentially associated with low Hg or Pb exposure.[21] Among different Hg species, MeHg is one of the most toxic forms. Keyvanshokooh *et al.*[22] had used 2-DE based techniques to determine the changes in the brain proteome of juvenile beluga (*Huso huso*) when exposed to dietary MeHg. They had found eight significantly differentially expressed proteins, which are implicated in cell metabolism, protein folding and cell division, in the brains of fishes.[22] In addition, proteomes of cultured mouse cerebellar granule cells[23,24] and human lymphocytes[25] exposed to MeHg have also been analyzed to dissect biochemical pathways of MeHg toxicity.

The whole set of proteomic data can facilitate our understanding of the biological processes in response to Hg and other heavy metal exposure. Nevertheless, a conventional proteomic approach may overlook the metalloproteins that only undergo alternation in metal-binding but have little change in expression when exposed to metals, or those have relatively low abundance in a proteome.[26] To partially address this problem, we and others have developed advanced nuclear analytical approaches to specifically study the distribution and composition of metalloproteins in a proteome, as well as the structural and functional characterization of metalloproteins.[27,28] For instance, laser ablation-inductively coupled plasma-mass spectrometry (LA-ICP-MS) had been used to identify metalloproteins in gels.[29] However, due to the limitations of LA (destructive, high cost, *etc.*), some non-destructive methods have been developed such as synchrotron radiation X-ray fluorescence spectroscopy (SRXRF). With SRXRF, metal-binding proteins can be readily detected with high sensitivity in 2-DE gels. This method had been employed to identify metalloproteins in sweet orange (*Citrus sinensis* L. Osbeck)[30] and human liver tissues[31,32] (reviewed by Shi and Chance[28]). In this study, we took *E. coli* as a simple model organism to identify the change in metalloproteome under Hg stress. Proteomic and metalloproteomic analyses of *E. coli* upon exposure to 15 μM $HgCl_2$ have been carried out. Hg^{2+} induced differentially expressed proteins and Hg-containing proteins have been identified. Mechanisms of cellular adaptation and compensation against Hg^{2+} toxicity have also been discussed. Our results provided clues about which proteins might be implicated in the cellular response of *E. coli* to Hg^{2+} on a proteome scale.

Materials and methods

Tryptone and yeast extract were purchased from Oxoid (Basingstoke, UK); ampicillin, dithiothreitol (DTT) and 3-[(3-cholamidopropyl)-dimethylammonio]-1-propanesulfonate (CHAPS) from Merck (Darmstadt, Germany); urea, Tris, sodium dodecyl sulfate (SDS) and iodoacetamide from Sigma (St Louis, USA); ampholyte from Academy of Military Medical Science (Beijing, China); acetic acid and methanol from Guoyao (Beijing, China) were of analytical purity. All the solutions were prepared with ultrapure water (18.2 MΩ cm^{-1}) obtained from Milli-Q and then stored at 4 °C or −20 °C.

E. coli culture and its growth curve

E. coli was grown in LB medium (1% of tryptone, 0.5% of yeast extraction, 1% of NaCl and 50 μg mL^{-1} of ampicillin, pH 7.2) at 37 °C with shaking at 220 rpm for about 9 h (the density is about 10^9 mL^{-1}). Then 100 μL culture was transferred to a fresh medium, supplemented with 15 μM $HgCl_2$ or 30 μM selenomethionine, and incubated at 37 °C with shaking at 220 rpm for 22 h (control or Se) or 40 h (Hg or Hg + Se) (Fig. 1). The growth curve of *E. coli* was obtained by taking absorbance measurements at 600 nm.

Protein extraction

Bacterial cells were harvested in their log phase by centrifugation at 5000 rpm for 15 min, 4 °C. The pellet was washed twice with Tris-HCl buffer (pH 8.0), followed by re-suspending in lysis buffer (7 M urea, 2 M thiourea, 1% DTT, 4% CHAPS, 2% ampholyte, 1 mM PMSF). Cell suspension was subjected to ultrasonic disruption (Xin Yi Biotechnology, China) in ice-bath for totally 7 min, 5 s each with 10 s interval. The mixture was centrifuged at 14 000 rpm, 4 °C, 20 min (Sigma, USA). The supernatant was collected and stored at −20 °C (temporary storage) or −80 °C (long storage) in small aliquots for further studies. Protein concentrations of the supernatant were determined using Bradford method.[33]

Separation of proteins with 2-DE and differential analysis of protein expression

2-DE was carried out to study the differential expression of proteins, as well as the detection of metal-containing proteins.

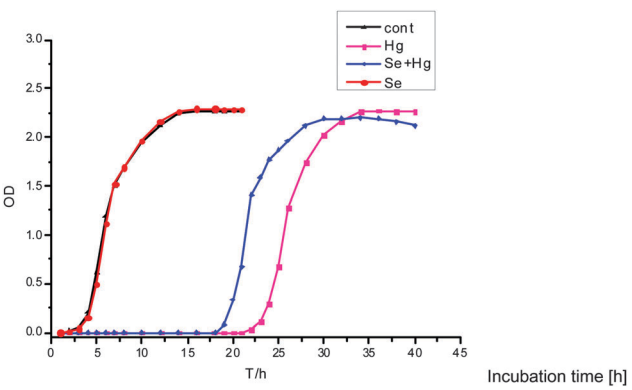

Fig. 1 Effects of Hg^{2+} and/or selenomethionine on the growth curve of *E. coli*. Cont: control *E. coli* grown without Hg^{2+} or selenomethionine; Hg: *E. coli* exposed to Hg^{2+}; Se: *E. coli* exposed to selenomethionine; Se + Hg: *E. coli* exposed to both Hg^{2+} and selenomethionine.

Isoelectric focusing (IEF) was performed using 7 cm immobilized pH gradient (IPG) strips with a linear pH gradient from 5 to 8 in a Bio-Rad IEF cell. IPG strips were rehydrated passively for 16 h with rehydration buffer (7 M urea, 2 M thiourea, 4% CHAPS, 65 mM DTT, 0.2% ampholyte, 0.001% bromophenol blue) premixed with the protein extracts (150 μg proteins per strip). IEF was run following a four-step program (250 V for 30 min, 500 V for 30 min, 4000 V for 3 h and 4000 V for 16 000 V h) at 18 °C. After IEF, the strips were equilibrated with gentle shaking in 2.5 mL equilibration buffer (6 M urea, 2% SDS, 0.375 M Tris-HCl pH 8.8, 20% glycerol) containing additionally 2% DTT for 15 min, and then in equilibration buffer with 2.5% iodoacetamide for another 15 min. Strips were transferred onto 1 mm thick 12% non-gradient SDS-polyacrylamide gel electrophoresis (SDS-PAGE) gels. SDS-PAGE was performed under ice-water cooling conditions using a two-step program, 60 V for 20 min, followed by 150 V until the tracking dye reached the bottom of the gel. Two parallel gels were run simultaneously. For detection of metal-containing proteins, SDS-PAGE gels were fixed with formaldehyde solution (containing 26% ethanol, 5% formaldehyde and 3% glycerol) as modified from Steck *et al.*,[34] and then dried using Gel Drier (Bio-Rad) at 80 °C for 90 min for subsequent elemental analysis. To identify proteins with differential expression, SDS-PAGE gels were stained with Coomassie brilliant blue (CCB) R-250. After staining, gel images were acquired using image scanner (Powerlook 2000XL-USB). Differential analysis was performed with PDQuest version 8.0 (Bio-Rad). After calibration, spot detection and background subtraction, the volume (area × intensity) of each spot was quantified. The total spot volume normalization method was applied in which the percentage of each spot volume on a gel is determined relative to the total volume of all spots on that gel. Then, differentially expressed proteins were identified by comparing the ratios of spot volumes between control and Hg^{2+} treated samples.

Elemental imaging of 2-DE gels by SRXRF

The elemental analysis of the 2-DE gels was modified from a previous report[31] and carried out at beam line 4W1B in Beijing Synchrotron Radiation Facility (BSRF). The storage ring ran at an energy of 2.5 GeV with a current intensity of 150–250 mA. Continuous synchrotron X-rays were monochromatized with a single multilayer monochromator. The incident beam was focused using Kirkpatrick–Baez Mirror to a size of 500 μm × 500 μm. In this study, the samples were mounted on an *X*–*Y* travelling stage. A monochromatic SR with photon energy of 13.5 keV was used to scan the 2-DE gels. The sample platform was moved at the *X* and *Y* directions with an interval of 1 mm for each step. The SRXRF signals were collected up to 45 s for each point with a Si (Li) detector. The fluorescence intensities were recorded and analyzed with multiple channel analyzers (MCA 4000). The peak areas of Se and Hg were normalized to that of Compton scattering for correcting the effect of SR beam flux variation on the signal intensity. Normalized peak counts were used to estimate the relative contents of elements.

Protein identification with ESI-MS/MS and peptide mass fingerprinting analysis

Protein spots excised from preparative gels were placed in Eppendorf tubes. Each gel piece was washed twice with Milli Q water for 5 min. Then the gel pieces were covered and incubated with 200 μL 50 mM NH_4HCO_3 in 33% (v/v) acetonitrile (ACN) at room temperature for 15 min, which was repeated until the blue dye became invisible. Subsequently, the gel pieces were dehydrated using 200 μL 50 mM NH_4HCO_3 in 50% ACN for 10 min and dried in a speed vacuum concentrator (Thermo, SC210A-115, USA). The extraction and enzymatic digestion of proteins were performed at 37 °C for 20 h after adding 20 μL 5 μg mL^{-1} trypsin solution (in 50 mM NH_4HCO_3) to the gel pieces. Tryptic peptide mixture was stored at −20 °C prior to nano liquid chromatography (LC)-ESI-Quadrupole time-of-flight MS/MS analysis. For identification of proteins, the obtained ion spectra were searched against Swiss-Prot database using the MASCOT search engine.

Results and discussion

Effects of Hg^{2+}/selenomethionine on *E. coli* growth

E. coli was cultured in LB media containing different concentrations of Hg^{2+}. When the concentration of Hg^{2+} is up to 20 μM, no bacterial growth could be observed in 48 h, while 10 μM Hg^{2+} is the lowest dosage with observable effect on bacterial growth. Thus, 15 μM Hg^{2+} was used to study cellular toxicity of Hg^{2+}. The effect of Hg^{2+} on the growth curve of *E. coli* is shown in Fig. 1. In order to investigate the effect of selenomethionine on Hg^{2+} toxicity, the *E. coli* with or without Hg^{2+} treatment was also exposed to 30 μM selenomethionine. Fig. 1 shows that the growth curve of selenomethionine-treated group has no significant difference from that of non-treated control. However, *E. coli* cultured in Hg^{2+}-containing medium has a lag phase of about 22 h compared to that of about 2 h in control or selenomethionine-containing medium. The delay in exponential phase indicates the toxic effects of Hg^{2+} on bacterial growth. When selenomethionine was added to Hg^{2+} containing medium, the lag time in bacterial growth is shortened to about 18 h, implying a possible antagonistic effect of selenomethionine on Hg^{2+} toxicity. As previously reported, an Hg–selenomethionine salt can be formed with low solubility in solution,[35] which may reduce the bioavailability of Hg^{2+} and account for attenuated Hg^{2+} toxicity in the presence of selenomethionine.

Differential analysis of protein expression

2-DE images representing protein profiles of *E. coli* are shown in Fig. 2. Spot volumes were determined by PDQuest. Differentially expressed proteins were defined as the proteins with at least 3-fold difference in spot volumes between Hg^{2+} exposure group and control in three independently repeated experiments. Fig. 2 shows five protein spots with significant difference in protein expression. One (spot no. 1) was down-regulated when *E. coli* was exposed to Hg^{2+}, whereas the others were up-regulated by Hg^{2+} (Table 1).

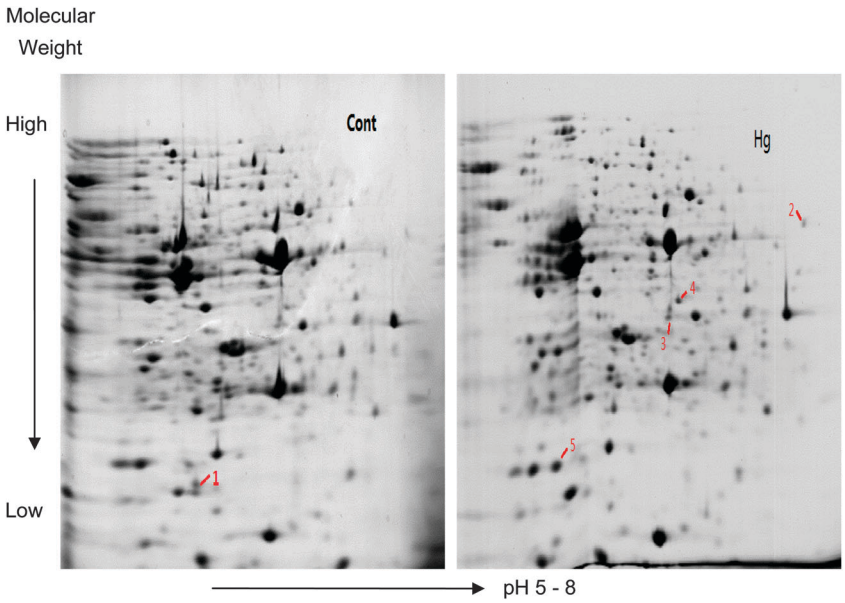

Fig. 2 2-DE CCB images of protein extracts from *E. coli*. Cont: control *E. coli* grown without Hg^{2+} or selenomethionine; Hg: *E. coli* exposed to Hg^{2+}. Spot 1: outer membrane protein W; spot 2: transcription termination factor rho; spot 3: cysteine synthase; spot 4: transaldolase A; spot 5: alkyl hydroperoxide reductase subunit C. Hg^{2+}-treated sample was subjected to SRXRF analysis.

Table 1 *E. coli* proteins of interest were identified by peptide mass fingerprinting analysis

Spot no.	Description	Sequence coverage (%)	Protein score	Nominal mass (Mr)	Calculated pI value
1	Outer membrane protein W	24	48	22 913	6.32
2	Transcription termination factor rho	40	310	47 032	6.75
3	Cysteine synthase	61	1008	34 525	5.83
4	Transaldolase A	64	367	35 865	5.89
5	Alkyl hydroperoxide reductase subunit C	27	768	20 862	5.03
6	Pyruvate kinase	32	1646	51 039	5.77

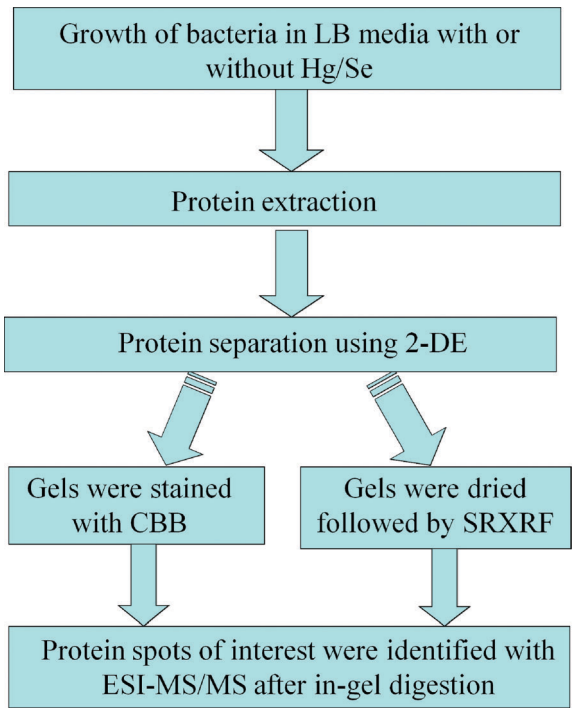

Scheme 1 A diagram illustrating the methodology used in this study.

Distribution of Hg/Se containing proteins in 2-DE gels

The 2-DE gels of *E. coli* grown in Hg-containing culture medium were subjected to SRXRF analysis after formaldehyde fixation (Scheme 1). The gels were not stained to avoid metal loss or staining chemicals which may interfere with SRXRF analysis. Hg^{2+}-treated sample and selenomethionine-treated sample were subjected to SRXRF analysis, respectively. A CBB-stained 2-DE gel of *E. coli* grown in Hg-containing culture medium and the distributions of Hg and Se in the unstained 2-DE gel are shown in Fig. 3. The area for SRXRF scan measurement is marked with a red rectangle in 2-DE gel. More than 20 Hg-containing spots were detected. The distribution of Se was also investigated due to a strong affinity between these two elements. At least 4 spots contain both Se and Hg (Fig. 3, marked with red circles). These proteins may be involved in the antagonism between Hg and Se *via* the formation of Hg–Se–S–protein complexes that had been previously reported.[36,37] By comparing the image of CBB-stained gel with SRXRF image, 6 Hg-containing spots could be correlated between these two images (Fig. 3, marked with blue squares), whereas the other Hg-containing spots could not be found in stained gel. The discrepancy between two protein detection methods may be due to the relatively low expression of some Hg-containing proteins that cannot be visualized by CBB staining. It can be seen from Fig. 3 that metal distribution is not very consistent with CBB-stained

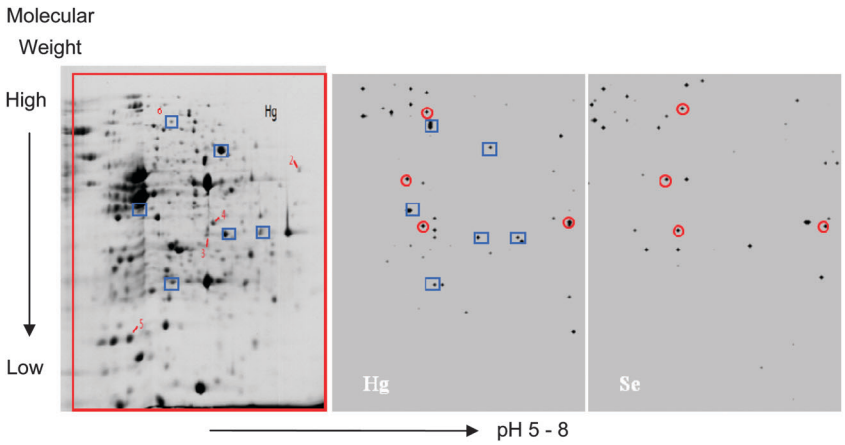

Fig. 3 Distribution of Hg and Se in 2-DE gels detected with SRXRF. Left panel: CCB image of Hg^{2+}-treated sample; middle panel: SRXRF image of Hg^{2+}-treated sample; right panel: SRXRF image of selenomethionine-treated sample. Red circles represent the spots containing both Hg and Se; blue squares denote the proteins containing only Hg in 2-DE gels. Spot 6: pyruvate kinase.

protein profile. It thus suggested that SRXRF may offer a more sensitive detection of metal-containing proteins in a proteome.

Hg is an unusual metal in terms of forming very stable covalent bonds with thiols that can even survive the LC-MS/MS process.[38,39] Its stable isotope distribution has been used to identify the Hg protein modifications in whole proteomes with LC-MS/MS.[40] Similarly, selenium can also be incorporated into peptide chains in forms of selenomethionine or selenocysteine. Therefore, it is acceptable to separate Se or Hg-containing proteins with denaturing 2-DE. A native 2-DE procedure will be required for separation of proteins binding weakly to other metals to avoid the metal loss arising from denaturing electrophoresis conditions.

Hg^{2+} has a particularly high affinity for thiols and can undergo a rapid exchange between different thiol groups. It is possible that the thiol groups in some proteins, which are not accessible inside the cells, may be exposed to Hg^{2+} when cells are lysed. In addition, DTT which contains thiol groups was used as a reducing agent for protein extraction and separation in this study. DTT can either compete with proteins for Hg^{2+} binding or form a DTT–Hg–protein complex.[41] Therefore, some (but not all) Hg-binding proteins may elude the SRXRF identification due to Hg loss in the presence of DTT. Taken together, Hg-containing proteins identified *in vitro* may not represent a full list of bona fide Hg-binding proteins inside the cells. Following *in vitro* profiling, the validation of Hg-binding proteins in intact cells is needed.

Response of *E. coli* to Hg^{2+} exposure

The differentially expressed proteins and the Hg-binding proteins were identified using ESI-MS/MS and peptide mass fingerprinting analysis. Proteins exhibiting significant spot volume variation associated with Hg^{2+} exposure were identified as outer membrane protein W (OmpW), transcription termination factor rho (Rho), cysteine synthase, transaldolase A and alkyl hydroperoxide reductase subunit C (AhpC). An Hg-binding protein (Fig. 3, spot no. 6) was identified as pyruvate kinase, whose expression is not significantly altered by Hg^{2+}. Detailed information of mass spectrometry and peptide mass fingerprinting analysis is shown in Table 1.

Our results showed that OmpW is down-regulated in *E. coli* when exposed to Hg^{2+}. OmpW is widely present in Gram-negative bacteria and belongs to an outer membrane protein family. The crystal structure of OmpW protein indicated that there is a protein channel for transport of small compounds across the bacterial outer membrane.[42] The expression of OmpW protein is dependent on culture conditions such as temperature, salinity, and availability of oxygen. Reduction in OmpW expression had been detected under elevated temperature, high salt concentration and low aeration, suggesting that the modulation of OmpW expression by environmental factors may be linked to the adaptive response of the organism under stress conditions.[43,44] Furthermore, OmpW is also involved in osmoregulation.[45,46] In this study, OmpW expression is dramatically decreased in *E. coli* when exposed to Hg^{2+}, which is consistent with Cr^{6+} or Zn^{2+} mediated down-regulation of OmpW expression in *E. coli*.[47,48] We propose that OmpW may be associated with osmosis of Hg^{2+} in that down-regulation of OmpW expression reduces cellular uptake of Hg^{2+} to pull the bacteria through Hg stress. In addition, our study also demonstrated that supplying selenomethionine to Hg-containing medium results in a less down-regulation of OmpW expression (unpublished data), which may account for the antagonism of selenomethionine against Hg^{2+} toxicity.

Hg^{2+} exposure induces the expression of cysteine synthase, implying an elevated cysteine level in *E. coli*. Cysteine synthesis is a prerequisite to the biosynthesis of cysteine-containing proteins. As we know, Hg is a thiophilic element and thus the biological activity of Hg is generally related to its binding to cysteine residues in proteins or peptides. It has been reported that Hg^{2+} exposure can induce the synthesis of metallothioneins (MT) in neurons.[49,50] MTs are cysteine-rich proteins and widely exist in bacteria, fungi, plants and eukaryotes. MT proteins typically have one or two domains, which can be bound to

multiple monovalent or divalent metal ions.[51] Elevated concentrations of MTs in tissues reduce the toxic effects of mutagens and heavy metals. In this study, we found Hg^{2+}-induced increase in expression of cysteine synthase, which may indirectly facilitate the biosynthesis of cysteine-rich proteins, such as MTs, to quench free Hg^{2+} in the cells.

AhpC is another protein whose expression is induced by Hg^{2+}. AhpC encodes subunit C of alkyl hydroperoxide reductase, an enzyme that reduces alkyl hydroperoxides to the corresponding alcohols. AhpC homologs are widely present in prokaryotes, and AhpC is about 40% identical to thioredoxin peroxidase from yeast, plants, amoebae, nematodes, rodents, and humans.[52] Therefore, homologs of AhpC belong to a large family of antioxidant proteins existing in organisms from prokaryotes to humans.[53] Hg^{2+} exposure can produce free radicals, leading to oxidation of lipids, DNA and proteins.[6,8,54] For instance, oxidation of lipids produces aldehyde and hydroperoxide. When *E. coli* is exposed to Hg^{2+}-containing medium, a high level of hydroperoxide could be produced. In this regard, overexpression of AhpC may help *E. coli* to cope with Hg stress by removing the toxic side product (hydroperoxides).

Besides differentially expressed proteins, an Hg-containing protein was identified as pyruvate kinase by ESI-MS/MS. Pyruvate kinase is a rate-limiting enzyme involved in glycolysis. It catalyzes the transfer of a phosphate group from phosphoenolpyruvate to ADP, producing a molecule of pyruvate and an ATP, which is the final step in the glycolytic pathway. Yeast homolog of pyruvate kinase consists of four subunits, each of which contains six cysteine residues. One thiol group in cysteine residue lies in the active site, and its substitution leads to irreversible inactivation of the enzyme. Another thiol group is part of the allosteric site of the enzyme, and its substitution causes reversible inactivation due to a protein conformational change.[55] It has been reported that administration of Hg^{2+} solution inhibits the activity of thymic pyruvate kinase in mice.[56] In this study, we found that pyruvate kinase is bound to Hg, presumably due to the high affinity of SH group for Hg. Taken together, these data may suggest a direct inactivation of pyruvate kinase by binding of Hg to the active or allosteric site of the enzyme.

When pyruvate kinase is inactivated by Hg, other compensating pathways could be activated to maintain glycometabolic balance. It is worthy of note that transaldolase A, an enzyme in pentose phosphate pathway,[57] is overexpressed in *E. coli* upon Hg^{2+} exposure in this study. The last overexpressed protein, *i.e.* Rho, is an essential protein in prokaryotes involved in the termination of transcription by binding to the transcription terminator pause site.[58] When exposed to Hg^{2+} or/and selenomethionine, the protein was up-regulated. However, the association of Rho overexpression with Hg/Se exposure remains unclear and further investigation is thus needed.

Conclusions

SRXRF is an advanced nuclear analytical technique for metalloproteomics and offers a non-destructive approach for studying protein samples in gels. It can be used to identify and characterize the metal-binding proteins and metal-responding proteins when combined with 2DE/MS. By taking advantages of SRXRF-based metalloproteomic and proteomic approaches, we investigated the cellular response of *E. coli* upon Hg^{2+} exposure. Our results suggested that expression of OmpW, a protein associated with penetrability of exogenous molecules, is implicated in Hg^{2+} toxicity. The biosynthesis of AhpC is promoted by the Hg^{2+} exposure, resulting in an activation of antioxidant system. In addition, an Hg-binding protein, *i.e.* pyruvate kinase, which eluded detection by conventional proteomic approach, was identified by SRXRF-based method. This study thus highlighted the great potential of metalloproteomic study in providing additional information for proteomics.

Acknowledgements

This work was financially supported by National Natural Science Foundation of China (Grant Nos. 20931160430, 20777075, 21271059), National Basic Research Program of China (No. 2011CB933101), IHEP Innovation program (No. Y2515560U1) and research Fund for the Doctoral Program of Higher Education of China (No. 20111301110004). We thank Dongliang Chen and other staff members of 4W1B (BSRF) for their assistance during the SRXRF measurement.

References

1 S. Balshaw, J. Edwards, B. Daughtry and K. Ross, *Rev. Environ. Health*, 2007, **22**, 91–113.
2 O. Lindqvist, K. Johansson, M. Aastrup, A. Andersson, L. Bringmark, G. Hovsenius, L. Håkanson, Å. Iverfeldt, M. Meili and B. Timm, *Water, Air, Soil Pollut.*, 1991, **55**, 1–261.
3 P. Holmes, K. A. James and L. S. Levy, *Sci. Total Environ.*, 2009, **408**, 171–182.
4 J. K. Virtanen, T. H. Rissanen, S. Voutilainen and T. P. Tuomainen, *J. Nutr. Biochem.*, 2007, **18**, 75–85.
5 N. Ercal, H. Gurer-Orhan and N. Aykin-Burns, *Curr. Top. Med. Chem.*, 2001, **1**, 529–539.
6 T. W. Clarkson, *Crit. Rev. Clin. Lab. Sci.*, 1997, **34**, 369–403.
7 B. Hultberg, A. Andersson and A. Isaksson, *Toxicology*, 2001, **156**, 93–100.
8 B. O. Lund, D. M. Miller and J. S. Woods, *Biochem. Pharmacol.*, 1993, **45**, 2017–2024.
9 K. Jomova and M. Valko, *Toxicology*, 2011, **283**, 65–87.
10 K. Rahman, *Clin. Interventions Aging*, 2007, **2**, 219–236.
11 D. Cargnelutti, L. A. Tabaldi, R. M. Spanevello, G. de Oliveira Jucoski, V. Battisti, M. Redin, C. E. Linares, V. L. Dressler, E. M. de Moraes Flores, F. T. Nicoloso, V. M. Morsch and M. R. Schetinger, *Chemosphere*, 2006, **65**, 999–1006.
12 J. Perottoni, L. P. Lobato, A. Silveira, J. B. Rocha and T. Emanuelli, *Environ. Res.*, 2004, **95**, 166–173.
13 L. Su, M. Wang, S. T. Yin, H. L. Wang, L. Chen, L. G. Sun and D. Y. Ruan, *Ecotoxicol. Environ. Saf.*, 2008, **70**, 483–489.
14 A. Fanous, W. Weiss, A. Görg, F. Jacob and H. Parlar, *Proteomics*, 2008, **8**, 4976–4986.

15 R. A. Bradshaw and A. L. Burlingame, *IUBMB Life*, 2005, **57**, 267–272.
16 Y. Hu, G. Wang, G. Y. Chen, X. Fu and S. Q. Yao, *Electrophoresis*, 2003, **24**, 1458–1470.
17 Y. Hu, X. Huang, G. Y. Chen and S. Q. Yao, *Mol. Biotechnol.*, 2004, **28**, 63–76.
18 Y. A. Chen, W. C. Chi, T. L. Huang, C. Y. Lin, T. T. Quynh Nguyeh, Y. C. Hsiung, L. C. Chia and H. J. Huang, *Plant Physiol. Biochem.*, 2012, **55**, 23–32.
19 P. Isarankura-Na-Ayudhya, C. Isarankura-Na-Ayudhya, L. Treeratanapaiboon, K. Kasikun, K. Thipkeaw and V. Prachayasittikul, *Eur. J. Sci. Res.*, 2009, **25**, 679–688.
20 F. Marsano, L. Boatti, E. Ranzato, M. Cavaletto, V. Magnelli, F. Dondero and A. Viarengo, *J. Proteome Res.*, 2010, **9**, 2839–2854.
21 R. E. Birdsall, M. P. Kiley, Z. M. Segu, C. D. Palmer, M. Madera, B. B. Gump, J. A. MacKenzie, P. J. Parsons, Y. Mechref, M. V. Novotny and K. G. Bendinskas, *J. Proteome Res.*, 2010, **9**, 4443–4453.
22 S. Keyvanshokooh, B. Vaziri, A. Gharaei, F. Mahboudi, A. Esmaili-Sari and M. Shahriari-Moghadam, *Comp. Biochem. Physiol., Part D: Genomics Proteomics*, 2009, **4**, 243–248.
23 I. Vendrell, M. Carrascal, M. T. Vilaró, J. Abián, E. Rodríguez-Farré and C. Suñol, *Hum. Exp. Toxicol.*, 2007, **26**, 263–272.
24 I. Vendrell, M. Carrascal, F. Campos, J. Abián and C. Suñol, *Toxicol. Appl. Pharmacol.*, 2010, **242**, 109–118.
25 K. Das, U. Siebert, A. Gillet, A. Dupont, C. Di-Poï, S. Fonfara, G. Mazzucchelli, E. De Pauw and M. C. De Pauw-Gillet, *Environ. Health*, 2008, **7**, 52.
26 Y. Hu, G. Y. Chen and S. Q. Yao, *Angew. Chem., Int. Ed.*, 2005, **44**, 1048–1053.
27 Y. X. Gao, C. Y. Chen and Z. F. Chai, *J. Anal. At. Spectrom.*, 2007, **22**, 856–866.
28 W. Shi and M. R. Chance, *Cell. Mol. Life Sci.*, 2008, **65**, 3040–3048.
29 C. C. Chéry, D. Günther, R. Cornelis, F. Vanhaecke and L. Moens, *Electrophoresis*, 2003, **24**, 3305–3313.
30 F. M. Verbi, S. C. Arruda, A. P. Rodriguez, C. A. Pérez and M. A. Arruda, *J. Biochem. Biophys. Methods*, 2005, **62**, 97–109.
31 Y. X. Gao, C. Y. Chen, Z. F. Chai, J. J. Zhao, J. Liu, P. Q. Zhang, W. He and Y. Y. Huang, *Analyst*, 2002, **127**, 1700–1704.
32 Y. B. Liu, L. N. Li, Y. X. Gao, C. Y. Chen, B. Li, W. He, Y. Y. Huang and Z. F. Chai, *Hepatogastroenterology*, 2007, **54**, 2291–2296.
33 M. M. Bradford, *Anal. Biochem.*, 1976, **72**, 248–254.
34 G. Steck, P. Leuthard and R. R. Bürk, *Anal. Biochem.*, 1980, **107**, 21–24.
35 G. Feroci, R. Badiello and A. Fini, *J. Trace Elem. Med. Biol.*, 2005, **18**, 227–234.
36 J. Gailer, G. N. George, I. J. Pickering, S. Madden, R. C. Prince, E. Y. Yu, M. B. Denton, H. S. Younis and H. V. Aposhian, *Chem. Res. Toxicol.*, 2000, **13**, 1135–1142.
37 K. T. Suzuki, C. Sasakura and S. Yoneda, *Biochim. Biophys. Acta*, 1998, **1429**, 102–112.
38 F. M. Rubino, C. Verduci, R. Giampiccolo, S. Pulvirenti, G. Brambilla and A. Colombi, *J. Am. Soc. Mass Spectrom.*, 2004, **15**, 288–300.
39 Y. Guo, L. Chen, L. Yang and Q. Wang, *J. Am. Soc. Mass Spectrom.*, 2008, **19**, 1108–1113.
40 B. J. Polacco, S. O. Purvine, E. M. Zink, S. P. Lavoie, M. S. Lipton, A. O. Summers and S. M. Miller, *Mol. Cell. Proteomics*, 2011, **10**, M110.004853.
41 G. C. Benison, P. Di Lello, J. E. Shokes, N. J. Cosper, R. A. Scott, P. Legault and J. G. Omichinski, *Biochemistry*, 2004, **43**, 8333–8345.
42 H. Hong, D. R. Patel, L. K. Tamm and B. van den Berg, *J. Biol. Chem.*, 2006, **281**, 7568–7577.
43 B. Nandi, R. K. Nandy, A. Sarkar and A. C. Ghose, *Microbiology*, 2005, **151**, 2975–2986.
44 Y. Wang, *Biochem. Biophys. Res. Commun.*, 2002, **292**, 396–401.
45 C. Xu, S. Wang, H. Ren, X. Lin, L. Wu and X. Peng, *Proteomics*, 2005, **5**, 3142–3152.
46 W. S. Hu, P. C. Li and C. Y. Cheng, *Antimicrob. Agents Chemother.*, 2005, **49**, 3955–3958.
47 D. F. Ackerley, Y. Barak, S. V. Lynch, J. Curtin and A. Matin, *J. Bacteriol.*, 2006, **188**, 3371–3381.
48 L. J. Lee, J. A. Barrett and R. K. Poole, *J. Bacteriol.*, 2005, **187**, 1124–1134.
49 K. K. Kramer, J. T. Zoelle and C. D. Klaassen, *Toxicol. Appl. Pharmacol.*, 1996, **141**, 1–7.
50 M. Aschner, T. Syversen, D. O. Souza and J. B. Rocha, *Exp. Biol. Med.*, 2006, **231**, 1468–1473.
51 M. Vasák, A. Galdes, H. A. Hill, J. H. Kägi, I. Bremner and B. W. Young, *Biochemistry*, 1980, **19**, 416–425.
52 H. Z. Chae, S. J. Chung and S. G. Rhee, *J. Biol. Chem.*, 1994, **269**, 27670–27678.
53 L. Chen, Q. W. Xie and C. Nathan, *Mol. Cell*, 1998, **1**, 795–805.
54 X. L. Jie, G. W. Jin, J. P. Cheng, W. H. Wang, J. Lu and L. Y. Qu, *Biomed. Environ. Sci.*, 2007, **20**, 84–89.
55 H. J. Wieker and B. Hess, *Hoppe-Seyler's Z. Physiol. Chem.*, 1972, **353**, 1877–1893.
56 M. P. Dieter, M. I. Luster, G. A. Boorman, C. W. Jameson, J. H. Dean and J. W. Cox, *Toxicol. Appl. Pharmacol.*, 1983, **68**, 218–228.
57 A. K. Samland and G. A. Sprenger, *Int. J. Biochem. Cell Biol.*, 2009, **41**, 1482–1494.
58 R. Shashni, S. Mishra, B. S. Kalayani and R. Sen, *Microbiology*, 2012, **158**, 1468–1481.